An aggregated dynamic flow model for pedestrian movement in railway stations

Flurin Hänseler

Bilal Farooq

Thomas Mühlematter

Michel Bierlaire

Transport and Mobility Lab, EPFL

April 2013

STRC | 13th Swiss Transport Research Conference

Monte Verità / Ascona, April 24 – 26, 2013

Transport and Mobility Lab, EPFL

An aggregated dynamic flow model for pedestrian movement in railway stations

Flurin Hänseler, Bilal Farooq, Thomas Mühlematter, Michel Bierlaire
{flurin.haenseler,bilal.farooq,thomas.muhlematter,michel.bierlaire}@epfl.ch

April 15, 2013

Abstract

Pedestrian flows occurring in train stations are multi-directional and highly non-stationary. In this work, we develop a cell-based pedestrian flow model capable of describing flow patterns arising when a multitude of trains arrive and depart in close succession. We assume that pedestrian demand, i.e., OD flows and corresponding route fractions, are known a priori. Based on first-order pedestrian flow theory and a cell-transmission model, propagation of individual groups of pedestrians is described depending on route, departure time and group size. Furthermore, traffic-dependent path choice is considered using route-specific potentials assigned to each cell. A detailed derivation of the mathematical framework and a literature review is provided, underlining the novel aspects of the proposed model.

Preliminary draft

Keywords
pedestrian flows, first-order traffic flow theory, cell transmission model, route choice, origin-destination demand, public transportation

1 Introduction

In peak hours, many railway stations are used at the limits of their capacity. While railway networks have been systematically extended in the past, pedestrian facilities in train stations have, at least in Switzerland, largely been neglected. Today, walkable areas are regularly congested during peak periods.

To better understand this phenomenon, we are developing a methodology for dynamically estimating pedestrian demand in train stations. Of importance in this framework is a pedestrian flow model, predicting walking times of pedestrian routes depending on prevailing traffic conditions.

In this study, we aim at developing a mesoscopic first-order traffic flow model. Such an approach allows to consider individual groups of pedestrians without the need of modeling the behavior of single agents. This is computationally cheap and desirable in the mentioned context. Individual characterization of travelers would be very complex, as the picture on the title page of this article might indicate.

The proposed traffic model combines a set of equations representing flow conservation, hydrodynamic theory and a characteristic fundamental diagram with a cell-based space representation. Governing equations are solved numerically in discrete time using finite differences. This approach is inspired by Daganzo's cell transmission model, initially developed for single-lane car traffic on highways (Daganzo, 1994).

2 Pedestrian propagation modeling

Before presenting an adapted version of Daganzo's cell transmission model for uni-directional pedestrian flow, this section gives a brief overview of relevant literature.

2.1 Network-based pedestrian propagation models

For estimating pedestrian walking times of aggregated groups of pedestrians, mainly three approaches have been considered: (i) models based on continuum theory for pedestrian flows (Hughes, 2002, Xia *et al.*, 2008), (ii) cell transmission models (Daganzo, 1994, Asano *et al.*, 2006), and (iii) queueing network based models (Løvås, 1994, Cheah and Smith, 1994).

Continuum theory for pedestrians is formulated as a partial differential equation, in which flow direction is defined by one or several potential fields. It is mostly used for evacuation simulations, where only a small number of origin-destination flows need to be considered.

Both cell transmission model (CTM) and queueing network based model (QNM) use a graph-based representation of space. CTM is a deterministic finite difference approximation of first-order flow theory, consisting of a flow conservation and a density-speed relation. QNM is based on random queueing processes and can be either approximated analytically in static problems (Cheah and Smith, 1994), or by simulation (Løvås, 1994, Daamen, 2004).

In CTM, pedestrians are considered as aggregated groups. Each group is characterized by its departure time and route. As it is deterministic, CTM is computationally less expensive than most simulators. It can incorporate empirical, statistically obtained relations between characteristic flow parameters. Such relations are usually referred to as fundamental diagram and are discussed in the next section. A challenge associated with applying CTM to pedestrian flows consists in finding an adequate software architecture that tracks propagation of people along their chosen trajectory.

QNM is disaggregate, i.e., propagation of agents along their route is described individually. Due to the microscopic nature of QNM, it is straight forward to consider agent-specific routes. Stochasticity introduced by random queueing processes makes a simulator necessary, which is costly. Çetın (2005) reports that accurate modeling of backward traveling jam waves using QNM can hardly be achieved. Guaranteeing a ‘fair’ behavior in pedestrian intersections seems possible, but is far from trivial (Charypar, 2008).

In this work, we pursue primarily a CTM-based approach, combining it with the concept of cell potentials for path choice. In future work, QNM components might be useful for modeling boarding and disembarkation processes. An example of QNM describing interactions between public transportation vehicles and pedestrians can be found in Daamen and Hoogendoorn (2007).

2.2 Fundamental diagrams for pedestrian flows

In this work, we employ empiric density-velocity relations, which represent the most prevalent type of fundamental diagrams for pedestrian flows.

Fundamental diagrams for unidirectional pedestrian flow are well established (Hankin and Wright, 1958, Mōri and Tsukaguchi, 1987, Weidmann, 1993, Seyfried *et al.*, 2005, Helbing *et al.*, 2007). For bi-directional counter flow, besides theoretical results with limited use in practice, only empiric point-to-point comparisons exist (Oeding, 1963, Older, 1968, Navin and Wheeler, 1969). A reason is that for bidirectional flow, speed not only depends on density, but also on flow composition.

For cross-flows as well as other multidirectional flows, studies are very scarce for the same reason as above (Tregenza, 1976, Daamen and Hoogendoorn, 2007). Fruin (1971) notes that the decrease in speed from unidirectional to multidirectional flow patterns is small, especially at low density. Obviously, this decrease not only depends on joint density, but also on flow ratio, which leads to a complexity that makes such laws largely impractical.

According to Weidmann (1993), average pedestrian speed in public spaces depends on density as follows

$$v(k) = v_m \left\{ 1 - \exp\left[-\gamma \left(\frac{1}{k} - \frac{1}{k_M} \right) \right] \right\}, 0 \leq k \leq k_M \tag{1}$$

where v_m denotes free flow speed (typically 1.34 m/s), γ is a shape parameter (1.913 #/m^2), and k_M represents jam density (5.4 #/m^2). Buchmüller and Weidmann (2008) provide a set of parameter values calibrated for pedestrian flows on stairs, ramps, as well as for corridors and other facility elements.

Tregenza (1976) proposed an alternative density-flow relation

$$v(k) = v_m \exp\left[-(k/\beta)^{\zeta} \right], k \geq 0 \tag{1'}$$

where free flow speed in a multi-directional flow field is estimated at $v_m = 1.68$ m/s, with $\beta = 1.87$ #/m^2 and $\zeta = 1.11$ (parameters estimated from Cheah and Smith, 1994, Fig. 3). In this relation, there is no hard capacity constraint, and velocity decreases exponentially with density. Different curves for uni-, counter- and multi-directional flows are reported, which differ for densities above $k \geq 1$ #/m^2. Figure 1 shows the fundamental diagrams according to Weidmann and Tregenza for a large density range.

2.3 First-order pedestrian flow theory

First-order traffic theory is a continuum theory developed for one-dimensional flow. It combines the use of a conservation principle with a fundamental diagram.

In uni-directional flow, conservation is expressed by means of a one-dimensional continuity equation

$$\frac{\partial q(x,t)}{\partial x} = -\frac{\partial k(x,t)}{\partial t} \tag{2}$$

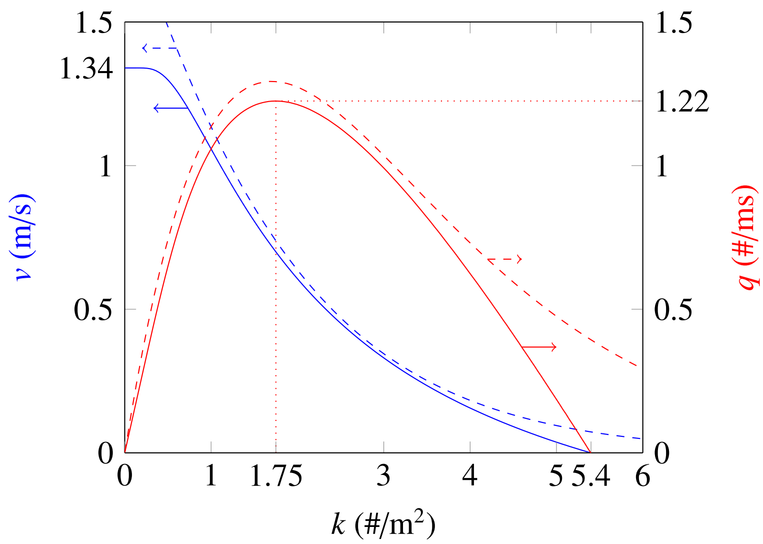

Figure 1: Average pedestrian speed (blue) and specific flow (red) as function of density according to Weidmann (1993, solid) and Tregenza (1976, dashed).

where x denotes space, t time, q flow and k line density. From hydrodynamic theory, it holds that

$$q(x,t) = kv(k) \tag{3}$$

where a density-velocity relation of the form $v(k)$ has been assumed. Two relations of this kind have been presented in the form of equations 1 and 1'.

2.4 Uni-directional pedestrian cell transmission model

The cell transmission model (Daganzo, 1994, CTM) numerically solves the set of equations comprised by first-order flow theory by applying finite differences on equation 2 and neglecting higher order terms $O(\Delta L^2)$, $O(\Delta T)$

$$\frac{q(x+\Delta L/2) - q(x-\Delta L/2)}{\Delta L} = -\left(\frac{k(x,t+\Delta T) - k(x,t)}{\Delta T}\right) \tag{4a}$$

Space and time is discretized into uniform cells of length ΔL, denoted by $\xi_i = [(i-1/2)\Delta L, (i+1/2)\Delta L]$ and uniform intervals of length ΔT, $\tau_j = [(j-1/2)\Delta T, (j+1/2)\Delta T]$, respectively. The time step is set to the free-flow travel time required for a pedestrian to traverse a cell,

$$\Delta T = \frac{\Delta L}{v_m}. \tag{4b}$$

In discrete space, the number of agents contained by cell ξ during time interval τ is given by

$$n_\xi(\tau) = \frac{1}{\Delta T} \iint_{\xi,\tau} k(x,t)dxdt \approx \Delta L k(x,t), t \in \tau, x \in \xi \tag{4c}$$

Number of agents exchanged between cell i and cell $i+1$ during time interval τ is given by

$$Q_i(\tau) = \int_\tau q\left((i+1/2)\Delta L, t\right) dt \approx \frac{\Delta L}{v_m} q\left((i+1/2)\Delta L, t\right), t \in \tau \tag{4d}$$

It is assumed that density at the interface between any two consecutive cells i and $i+1$ is determined by the preceding cell, i.e., $k((i+1/2)\Delta L, t) \approx n_i(\tau)/\Delta L$, $t \in \tau$. In discrete space, the continuity equation reads as

$$\frac{v_m}{\Delta L} \frac{Q_i(\tau) - Q_{i-1}(\tau)}{\Delta L} = -\frac{1}{\Delta L} \frac{n_i(\tau+1) - n_i(\tau)}{\Delta T} \tag{5a}$$

where equations 4a, 4c, 4d have been used. A rearrangement of terms yields

$$n_i(\tau+1) = n_i(\tau) + Q_i(\tau) - Q_{i+1}(\tau) \tag{5b}$$

Hydrodynamic cell flow depends on the choice of the fundamental diagram. Following the Weidmann-relation, it reads as

$$Q_i(\tau) = n_i(\tau) \left\{ 1 - \exp\left[-\gamma A \left(\frac{1}{n_i(\tau)} - \frac{1}{N} \right) \right] \right\} \tag{5c}$$

where equations 3 and 4d have been used, $N = k_M A$ denotes cell capacity, and A is the cell area. Adopting the fundamental diagram suggested by Tregenza, hydrodynamic cell flow is given by

$$Q_i(\tau) = n_i(\tau) \exp\left[-\left(\frac{n_i(\tau)}{A\beta} \right)^\zeta \right] \tag{5c'}$$

Recursion of CTM for Weidmann's fundamental diagram reads as

$$n_i(\tau+1) = n_i(\tau) + y_i(\tau) - y_{i+1}(\tau) \tag{6a}$$

where actual cell flow is given by

$$y_i(\tau) = \min\left\{ n_{i-1}(\tau), Q_i(\tau), \delta(N - n_i(\tau)) \right\} \tag{6b}$$

The three terms in brackets represent a non-negativity, a hydrodynamic, and a cell capacity constraint. Parameter δ determines the speed at which empty slots for agents travel backwards, i.e., the speed at which occupied space is released in a cell. Using Tregenza's relation, actual cell flow reduces to

$$y_i(\tau) = \min\{n_{i-1}(\tau), Q_i(\tau)\} \tag{6b'}$$

as the capacity constraint is not required by the corresponding fundamental diagram.

3 Multi-directional pedestrian propagation model

In a railway station, pedestrian flows are to a large extent multi-directional. A uni-directional CTM can therefore not be applied. Based on recent achievements in literature, we propose below two cell-based pedestrian propagation models which are more appropriate for extended walking areas. First, a model is discussed which describes flow patterns arising when the path of each pedestrian is known a priori. Subsequently, a second model is presented which allows for local path choice, i.e., pedestrians are able to make small detours to avoid regions of high traffic.

3.1 Review of cell-based pedestrian flow models

There are only a handful of cell-based models available that consider pedestrian flows at the aggregate level, i.e., with groups of pedestrians as modeling objects.

Two early papers from the same group are due to Hanisch *et al.* (2003) and Tolujew and Alcalá (2004). Flows in large public buildings are modeled in the framework of an online control system. Pedestrians are assumed to move from one cell to the next at a constant speed, irrespective of traffic conditions. Cells are subdivided into three categories, namely sources, sinks and storages. Storage cells represent areas where pedestrians can wait, such as for example a check-in facility in a railway station. Propagation of people along their paths is tracked across time. Overall, the suggested concept is similar to CTM, but it lacks any demand-supply interaction.

Asano *et al.* (2006) adapted a CTM to consider multi-directional pedestrian movement. Like in hydrodynamic theory of car traffic, a trapezoidal fundamental diagram is used (Lighthill and Whitham, 1955, Richards, 1956). It might therefore be argued that resulting model dynamics resemble rather those of vehicular traffic than of pedestrian flows. Among the main contributions of this study are the development of an appropriate merging and diverging behavior in cells for multi-directional flows.

Guo *et al.* (2011) developed a method of predicting pedestrian route choice behavior and physical congestion during evacuation of indoor areas. An important feature of their model lies in the use of cell potentials to determine route choice behavior among pedestrians. Specifically, an algorithm is developed which considers both route distance to destination and congestion ahead to assign pedestrian flows in space. Speed of transmission across cells is assumed to depend only on 'internal obstacles', which are exogenous and therefore traffic-independent. The developed framework is able to describe propagation of multiple flows of pedestrians targeting different destinations.

The seminal work by Daganzo regarding CTM, the multi-directional update scheme of Asano *et al.* as well as the potential-based route choice framework by Guo *et al.* constitute the principle ground on which the aggregated dynamic flow model of this study is built.

3.2 Model with known paths

The purpose of the model outlined below is to dynamically estimate the distribution of pedestrians, depending on infrastructure and pedestrian demand. It is assumed that the path of each pedestrian is known a priori.

Walkable space is discretized into square cells ξ of size ΔL^2. The resulting network of cells is represented by a directed graph $\mathcal{G} = (\mathcal{V}, \mathcal{E})$, consisting of vertices $\xi \in \mathcal{V}$ and edges $g \in \mathcal{E}$ (cell gates). For each cell ξ, $\mathcal{O}(\xi)$ and $\mathcal{I}(\xi)$ denote the of outflow gates and inflow gates, respectively. Time is considered in discrete space $\mathcal{T}$ with uniform intervals $\tau \in \mathcal{T}$ of length $\Delta T = \Delta L / v_m$ like in the original CTM.

Let $\ell \in \mathcal{L}$ be a group of pedestrians, characterized by a path Γ, a departure time interval τ_0, and group size m_0. $\mathcal{L}$ denotes the ensemble of these groups. A path is defined as a sequence of cells with no loops. Furthermore, let $m_\ell(\xi, \tau)$ be the number of people belonging to group ℓ in cell ξ during time interval τ.

Like in the uni-directional model, hydrodynamic flow in cell ξ during interval τ is governed by a corresponding fundamental diagram. Weidmann's density-speed-relation yields

$$Q_\xi(\tau) = \sum_{\ell \in \mathcal{L}} m_\ell(\xi, \tau) \left\{ 1 - \exp\left[-\gamma_\xi A_\xi \left(\frac{1}{\sum_{\ell \in \mathcal{L}} m_\ell(\xi, \tau)} - \frac{1}{N_\xi} \right) \right] \right\} \tag{7}$$

where for cell-specific parameters (denoted by subscript ξ) the same notation is kept as hitherto. Free-flow speed v_m is a global system parameter, i.e., necessarily homogeneous across cells. Analogously, the hydrodynamic flow corresponding to Tregenza reads as

$$Q_\xi(\tau) = \sum_{\ell \in \mathcal{L}} m_\ell(\xi, \tau) \exp\left[- \left(\frac{\sum_{\ell \in \mathcal{L}} m_\ell(\xi, \tau)}{A_\xi \beta_\xi} \right)^{\zeta_\xi} \right] \tag{7'}$$

Flow between any two adjacent cells is determined by the sending capacity of the emitting link, and the receiving capacity of the target cell. This concept was originally developed by Daganzo (1995), has been modified by Asano *et al.* (2006) and is extended further below.

The sending capacity of gate $g \in O(i)$ corresponding to group ℓ during interval τ is defined as

$$S_g^\ell(\tau) = \min\left\{ m_\ell(i,\tau), \frac{m_\ell(i,\tau)}{\sum_{\ell \in \mathcal{L}} m_\ell(i,\tau)} Q_i(\tau) \right\} \tag{8}$$

Under free-flow conditions, all agents proceed from one cell to the next, and the non-negativity constraint (first term) is tight. In presence of 'link congestion', a demand-proportional supply distribution scheme is applied (second term). Similarly, the receiving capacity of cell j during interval τ is given by

$$R_j(\tau) = \min\left\{ \hat{Q}_j(\tau), \delta\left(N_j(\tau) - \sum_{\ell \in \mathcal{L}} m_\ell(j,\tau) \right) \right\} \tag{9a}$$

where the first restriction represents maximum cellular inflow, and the second a cellular capacity constraint (obsolete when using Tregenza's density-velocity relation). Maximum cellular inflow is a nodal performance characteristic, for which we propose

$$\hat{Q}_\xi(\tau) = \begin{cases} Q_{\xi,max} & \text{if } \sum_{\ell \in \mathcal{L}} m_\ell(\xi,\tau) \leq n_{\xi,max}, \\ Q_\xi(\tau) & \text{otherwise.} \end{cases} \tag{9b}$$

where $Q_{\xi,max}$ denotes maximum hydrodynamic flow and $n_{\xi,max}$ the corresponding cell occupation (i.e., the value at which equation 7 (or 7') attains its maximum).

The actual flow corresponding to group ℓ along gate $g : i \to j$ during interval τ is given by

$$y_g^\ell(\tau) = \begin{cases} S_g^\ell(\tau) & \text{if } \sum_{h \in \mathcal{I}(j)} \sum_{\ell \in \mathcal{L}} S_h^\ell(\tau) \leq R_j(\tau), \\ \frac{S_g^\ell(\tau)}{\sum_{k \in \mathcal{I}(j)} \sum_{\ell \in \mathcal{L}} S_k^\ell(\tau)} R_j(\tau) & \text{otherwise.} \end{cases} \tag{10}$$

Under free-flow conditions, all incoming pedestrians can be accommodated (first case), whereas in presence of 'cell congestion' again a demand-proportional supply distribution scheme is employed. For any group ℓ crossing consecutive gates $f : i \to \xi$, $g : \xi \to j$, flow balance in cell ξ during time interval τ yields

$$m_\ell(\xi, \tau+1) = m_\ell(\xi,\tau) + y_f^\ell(\tau) - y_g^\ell(\tau) \tag{11}$$

Equation 11 represents the main recursion of the multi-directional pedestrian propagation model with known paths. For source or sink cells, a similar recursion scheme can be derived. These cells have infinite capacity, and their hydrodynamic flow is determined exogenously.

3.2.1 Area-specific fundamental diagrams and virtual lanes

A limitation of the presented multi-directional CTM is its inability to allow for cell-specific density-velocity relations. In the above framework, free-flow speed is uniform across cells. This assumption is difficult to justify in pedestrian facilities of a transportation hub. For instance, on ramps or stairways, fundamental diagrams may not only differ across cells, but they are also anisotropic.

To relax this constraint, edge-specific update intervals are considered (Asano *et al.,* 2006). Free-flow travel time of a general edge g is given by

$$\Delta T_g = \frac{\Delta L_g}{v_{m,g}}$$

where ΔL_g and $v_{m,g}$ represent length and free-flow travel speed of edge g, respectively. In a heterogeneous update scheme, links may be considered in individual simulation intervals depending on their free-flow travel time.

In this approach, however, numerical dispersion is likely to occur at boundaries between differently clocked links: Let's assume it takes three simulation time steps to cross a certain link $g : i \to j$ under free flow conditions. This means that link g is considered every 3rd, 6th, 9th, . . . , time step. In this case, people having arrived in i at $\tau = 1$ or $\tau = 2$ are transmitted together, with different delays. Such an anomaly occurs at intersections between differently clocked sets of edges (e.g. at the beginning or the end of a ramp), but not within contiguous sets of links with uniform update cycle. When designing the network graph $\mathcal{G}$, total length of such boundaries should be kept as short as possible.

Besides cell-specific speed characteristics, parallel 'virtual lanes' between cells are conceivable as well (Tolujew and Alcalá, 2004). Fast walkers might for instance be assigned to priority lanes, and travelers with luggage to a slower edge. Like this, population heterogeneity can be considered by introducing characteristic attributes such as e.g. 'in a hurry' or 'handicapped'.

3.3 Model with known routes and local path choice

Previously, the notion of a path has been introduced. A path is as a sequence of cells without loops. A route, on the other hand, is a collection of different paths sharing the same sequence of 'related areas'. Let's illustrate this concept at the example of a railway station with two equivalent access ways to platforms. An arriving train passenger heading for an exit may choose between two routes, represented by either of the two access ways. The sequence of related areas is then either (platform P, access way A, exit E) or (platform P, access way B, exit E). No matter which route he chooses, he will have a variety of corresponding paths to choose from (e.g. shortest path, following a zigzag line, etc.). Within the chosen sequence of areas, i.e., the selected route, he may follow any path he desires.

In the model developed below, pedestrians can choose their path 'en route'. The choice is made based on local traffic conditions, conditioned by a potential field. Huang and Guo (2008) have developed an algorithm to derive such a potential field for pedestrian emergency simulations. Each cell is assigned several route-specific potentials. The potential increases with distance to destination, and is lower for cells with a higher degree of connectivity. A sample potential field illustrating this concept is shown in figure 2.

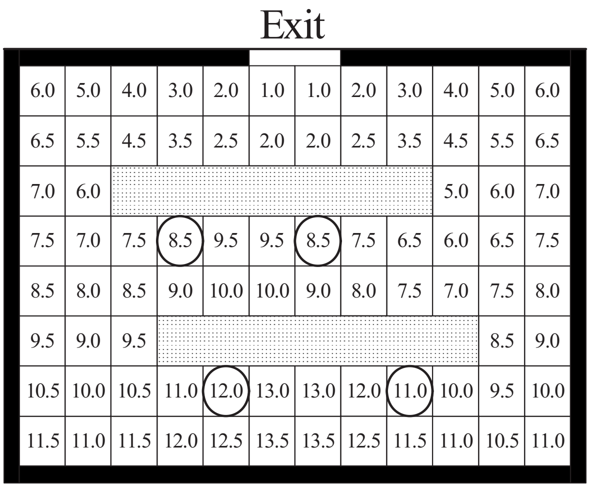

Figure 2: Example of a potential field for a room with a single destination, the exit, and two internal obstacles (shaded rectangles). Cell potentials reflect a measure of distance to the exit (Source: Huang and Guo, 2008, Fig. 2).

In the framework of the CTM with local path choice, a pedestrian group is characterized by a route R, departure time interval τ_0 and group size m_0. A route is defined by a directed graph $\mathcal{G}_R = (\mathcal{V}_R, \mathcal{E}_R)$, $\mathcal{G}_R \subseteq \mathcal{G}$, and a corresponding potential field, P_ξ^R, $\forall \xi \in \mathcal{V}_R$. If $\xi \notin \mathcal{G}_\mathcal{R}$, then $P_\xi^R = +\infty$.

Let's consider cell $\xi \in \mathcal{V}_R$, and let Φ_ξ^R and Θ_ξ^R be the set of links up- and downstream of cell ξ corresponding to route R, respectively. Then, the proportion of people on cell i on route R choosing edge $g : i \to j$ can for instance be expressed as (Guo *et al.*, 2011)

$$D_g^R(\tau) = \begin{cases} \frac{(P_i^R - P_i^R)\left[N_j(\tau) - \sum_{\ell \in \mathcal{L}} m_\ell(j,\tau)\right]}{\sum_{k \in \Theta_i^R} \left\{(P_i^R - P_k^R)\left[N_k(\tau) - \sum_{\ell \in \mathcal{L}} n_k^\ell(\tau)\right]\right\}}, & g \in \Theta_i^R \\ 0, & \text{otherwise.} \end{cases} \tag{12}$$

If Tregenza's fundamental diagram is used, turning proportions can be defined as

$$D_g^R(\tau) = \begin{cases} \frac{(P_i^R - P_j^R) v\left(\sum_{\ell \in \mathcal{L}} m_\ell(j,\tau)/A_i\right)}{\sum_{k \in \Theta_i R}\left\{(P_i^R - P_k^R) v\left(\sum_{\ell \in \mathcal{L}} m_\ell(k,\tau)/A_k\right)\right\}}, & g \in \Theta_i^R \\ 0, & \text{otherwise.} \end{cases} \tag{12'}$$

For the sending capacity of group ℓ in cell i along edge $g : i \rightarrow j$, we have

$$S_q^\ell(\tau) = \min\left\{ D_g^{R_\ell}(\tau) m_\ell(i,\tau), \frac{D_g^{R_\ell}(\tau) m_\ell(i,\tau)}{\sum_{l \in \mathcal{L}} m_\ell(i,\tau)} Q_i(\tau) \right\} \tag{8*}$$

The expressions for receiving capacity and actual gate flow remain unchanged. A balance equation for group ℓ in cell ξ during time interval τ yields

$$m_\ell(\xi, \tau + 1) = m_\ell(\xi, \tau) + \sum_{h \in \Phi_\xi^R} y_h^\ell(\tau) - \sum_{g \in \Theta_\xi^R} y_g^\ell(\tau) \tag{11*}$$

In comparison to recursion 11, inflows and outflows from several adjacent cells need to be taken into account due to the possibility of path choice.

4 Conclusions

Pedestrian facilities of railway stations are often congested during peak hours. This may compromise level of service in terms of safety, time table stability or customer satisfaction. To better understand flow patterns arising in transportation hubs, we develop an aggregated dynamic pedestrian propagation model based on first-order flow theory. Such an approach is computationally cheap and can cope with complex and non-stationary situations involving a large number of pedestrians.

The proposed model considers space as a two-dimensional network of cells with uniform pedestrian density. Pedestrians are distinguished with respect to their route, departure time, and any further characteristic attribute such as 'in a hurry' or 'handicapped'. Between any two adjacent cells, flow propagation is calculated based on the outflow capacity of the emitting cell and the inflow capacity of the receiving cell. Using this concept, propagation of pedestrians is estimated dynamically in discrete time. In presence of congestion, a demand-proportional supply distribution is applied to allocate flows to cells.

The resulting flow propagation scheme allows for i) cell- and direction-specific flow speeds (important on e.g. inclined areas), ii) separate 'lanes' for particular groups of pedestrians, depending on the aforementioned 'characteristic attribute', and iii) *en route* path choice depending on prevailing traffic conditions.

To demonstrate the validity of our model, we are currently investigating a counter- and cross-wave scenario at the example of a longitudinal corridor and an orthogonal intersection, respectively. This will allow to elucidate the different behavior under free-flow conditions and in presence of congestion. Subsequently, a real case study will be considered: For a large Swiss railway station, we dispose of comprehensive pedestrian tracking data. Dynamic origin-destination demand extracted from this data will be used as model input. Model prediction and actual data can then be directly compared to assess the applicability of the presented framework.

Acknowledgement

Financial support by SNF grant #200021-141099 'Pedestrian dynamics: flows and behavior' as well as by SBB-CFF-FFS in the framework of 'PedFlux' is gratefully acknowledged.

5 References

Asano, M., M. Kuwahara, A. Sumalee, S. Tanaka and E. Chung (2006) Pedestrian simulation considering stochastic route choice and multidirectional flow, paper presented at the *2nd International Symposium of Transport Simulation, EPFL, Switzerland*, 47–59.

Buchmüller, S. and U. Weidmann (2008) *Handbuch zur Anordnung und Dimensionierung von Fussgängeranlagen in Bahnhöfen*.

Çetın, N. (2005) Large-scale parallel graph-based simulations, Ph.D. Thesis, ETH Zürich.

Charypar, D. (2008) Efficient algorithms for the microsimulation of travel behavior in very large scenarios, Ph.D. Thesis, ETH Zürich.

Cheah, J. Y. and J. M. Smith (1994) Generalized M/G/c/c state dependent queueing models and pedestrian traffic flows, *Queueing Systems*, **15** (1) 365–386.

Daamen, W. (2004) Modelling passenger flows in public transport facilities, Ph.D. Thesis, Delft University of Technology.

Daamen, W. and S. Hoogendoorn (2007) Pedestrian free speed behavior in crossing flows, *Traffic and Granular Flow*, 299–304.

Daganzo, C. (1994) The cell transmission model: A dynamic representation of highway traffic consistent with the hydrodynamic theory, *Transportation Research Part B: Methodological*, **28** (4) 269–287.

Daganzo, C. (1995) The cell transmission model, Part II: Network traffic, *Transportation Research Part B: Methodological*, **29** (2) 79–93.

Fruin, J. J. (1971) Pedestrian planning and design, *Technical Report*.

Guo, R., H. Huang and S. Wong (2011) Collection, spillback, and dissipation in pedestrian evacuation: A network-based method, *Transportation Research Part B: Methodological*, **45** (3) 490–506.

Hanisch, A., J. Tolujew, K. Richter and T. Schulze (2003) Online simulation of pedestrian flow in public buildings, paper presented at the *Winter Simulation Conference*, vol. 2, 1635–1641.

Hankin, B. and R. Wright (1958) Passenger flow in subways, *OR*, **9** (2) 81–88.

Helbing, D., A. Johansson and H. Z. Al-Abideen (2007) Dynamics of crowd disasters: An empirical study, *Physical review E*, **75** (4) 046109.

Huang, H. and R. Guo (2008) Static floor field and exit choice for pedestrian evacuation in rooms with internal obstacles and multiple exits, *Physical Review E*, **78** (2) 021131.

Hughes, R. L. (2002) A continuum theory for the flow of pedestrians, *Transportation Research Part B: Methodological*, **36** (6) 507–535.

Lighthill, M. and G. Whitham (1955) On kinematic waves. II. A theory of traffic flow on long crowded roads, *Proceedings of the Royal Society of London. Series A. Mathematical and Physical Sciences*, **229** (1178) 317–345.

Løvås, G. (1994) Modeling and simulation of pedestrian traffic flow, *Transportation Research Part B: Methodological*, **28** (6) 429–443.

Mōri, M. and H. Tsukaguchi (1987) A new method for evaluation of level of service in pedestrian facilities, *Transportation Research Part A: General*, **21** (3) 223–234.

Navin, F. and R. Wheeler (1969) Pedestrian flow characteristics, *Traffic Engineering*, **39**.

Oeding, D. (1963) Verkehrsbelastung und Dimensionierung von Gehwegen und anderen Anlagen des Fußgängerverkehrs, Ph.D. Thesis, Bundesministerium für Verkehr, Abt. Strassenbau.

Older, S. (1968) *Movement of pedestrians on footways in shopping streets*, Traffic Engineering & Control.

Richards, P. (1956) Shock waves on the highway, *Operations research*, **4** (1) 42–51.

Seyfried, A., B. Steffen, W. Klingsch and M. Boltes (2005) The fundamental diagram of pedestrian movement revisited, *Journal of Statistical Mechanics: Theory and Experiment*, **2005** (10) P10002.

Tolujew, J. and F. Alcalá (2004) A mesoscopic approach to modeling and simulation of pedestrian traffic flows, paper presented at the *Proceedings of 18th European Simulation Multiconference*.

Tregenza, P. (1976) *The design of interior circulation*, Van Nostrand Reinhold.

Weidmann, U. (1993) *Transporttechnik der Fussgänger*, Institute for Transport Planning and Systems, ETH Zürich.

Xia, Y., S. Wong, M. Zhang, C.-W. Shu and W. H. Lam (2008) An efficient discontinuous galerkin method on triangular meshes for a pedestrian flow model, *International Journal for Numerical Methods in Engineering*, **76** (3) 337–350.